FACTA UNIVERSITATIS
Series: **Electronics and Energetics** Vol. 30, N^o 3, September 2017, pp. 327 - 350
DOI: 10.2298/FUEE1703327G

MODELLING SOLAR CELL S-SHAPED I-V CHARACTERISTICS WITH DC LUMPED-PARAMETER EQUIVALENT CIRCUITS - A REVIEW

Francisco J. García-Sánchez[1,2], Beatriz Romero[1], Denise C. Lugo-Muñoz[2,3], Gonzalo Del Pozo[1], Belén Arredondo[1], Juin J. Liou[3], Adelmo Ortiz-Conde[2]

[1]Superior School of Experimental Science and Technology (ESCET), Rey Juan Carlos University (URJC), Móstoles, Madrid 28933, Spain
[2]Solid State Electronics Laboratory (LEES), Simón Bolívar University (USB), Caracas 1080A, Venezuela
[3]EMOAT, LLC, 1933 Ayrshier Place., Oviedo, FL 32765, USA

Abstract. *This article reviews and appraises the dc lumped-parameter equivalent circuit models that have been proposed so far for representing some types of solar cells that can exhibit under certain circumstances a detrimental S-shaped concave deformation within the energy-producing fourth quadrant of their illuminated I–V characteristics. We first present a very succinct recollection of lumped-parameter equivalent circuits that are commonly used to model conventional solar cells in general. We then chronologically present and discuss lumped-parameter equivalent sub-circuits that, combined with conventional solar cell equivalent circuits, are used to specifically represent the undesired S-shaped behaviour. The mathematically descriptive equations of each complete equivalent circuit are also examined, and closed form solutions for the terminal current and voltage as explicit functions of each other are presented and discussed whenever available. While comparing the most salient features and explaining the practical advantages and disadvantages of such equivalent circuit models, we offer some comments on possible directions for further improvement.*

Key words: *Solar cell lumped-parameter equivalent circuit modelling, Solar cell concentrated-element equivalent circuit models, S-shaped current-voltage characteristics, S-shape kink, Organic solar cells, Lambert W function*

Received February 19, 2017
Corresponding author: Francisco J. García-Sánchez
Solid State Electronics Laboratory (LEES), Simón Bolívar University (USB), Caracas 1080A, Venezuela
(E-mail: fgarcia@ieee.org)

1. INTRODUCTION

The process of designing practical photovoltaic applications calls for the availability of dc lumped-parameter equivalent circuit models as simple as possible to compactly describe the solar cells' electric behaviour represented by their terminals' current–voltage (*I-V*) characteristics, measured in the dark and under standard illumination conditions. Solar cell lumped-parameter (or concentrated-element) equivalent circuit models ignore the spatial distribution of the electrical mechanisms present, and instead assume that they are concentrated and represented by certain idealized passive and active lineal and non-lineal electrical components, typically resistors, capacitors, inductors, diodes, and current voltage sources, located at certain positions in an electrical network. Under steady state (dc) conditions neither inductors nor capacitors are used. Such simple equivalent circuits constitute essential tools for photovoltaic systems simulation, as well as for the important task of advancing basic and applied research and technological development of emerging solar cells' materials, structures, and fabrication techniques.

Most well-established conventional solar cells under illumination exhibit the type of generic *I-V* characteristics that can be satisfactorily represented under steady state by the equivalent electrical behaviour of some of the conventional dc lumped-parameter circuit models that are shown in Fig.1 [1]. However, there are innovative developmental or still experimental solar cells, such as some of those based on binary and ternary compound semiconductors, non-crystalline hetero-junctions [2], novel silicon quantum dot solar cells [3], others based on perovskite semiconductors [4-6], and most notably organic semiconductor-based solar cells [7-9], that might exhibit under certain circumstances undesirable deformations of their illuminated *I-V* characteristics that impair their energy conversion capacity.

The main feature of such apparent anomaly becomes evident when the solar cell's *I-V* characteristics under illumination present a peculiar concave shape within the fourth quadrant (the power generating quadrant); instead of exhibiting the normally expected, so-called "J" type conventional convex shape. This deformation of the illuminated *I-V* curve is commonly referred to as the S-shape "kink" of the *I-V* characteristics [10]. The presence of such bend seriously reduces the solar cell's fill factor by depressing the location of the maximum power point, and thus represents a serious impairment for the cell's power conversion efficiency that must be avoided, minimised or suppressed [7, 11].

In the sections that follow we offer a chronological perspective view of the most relevant dc lumped-parameter equivalent circuit models that have been proposed to date, for specifically describing in a compact way this adverse S-shaped behaviour observed in the illuminated *I-V* characteristics of some otherwise promising solar cells.

2. SOLAR CELL EQUIVALENT CIRCUIT MODELS

The simplest possible mathematical description of the *I-V* characteristics at the terminals of any conventional solar cell measured under illumination conditions consists of adding a photo-generated current to the well known Shockley's ideal diode current equation [12]. The equation resulting from adding these two terms is an explicit compact model of the terminal current expressed as an exponential function of the terminal voltage. This simplest mathematical description of a solar cell electrical behaviour under

illumination represents a corresponding dc lumped-parameter equivalent circuit model that consists of the parallel combination of a diode and an illumination-dependent current source, as portrayed in Fig. 1(a).

Such descriptive mathematical representation is practically appealing, not only because of its compactness, but also because its explicit nature allows it to be easily inverted and numerically calculated. Unfortunately, this simplest model usually falls short of adequately describing all the relevant electrical phenomena that must be considered for solar cell development and photovoltaic system simulation and design. Thus, the corresponding very basic dc lumped-parameter equivalent circuit model shown in Fig. 1(a) is often deemed to be not accurate enough to be of practical use.

2.1. Conventional dc lumped-parameter circuit models

The basic equivalent circuit model is modified to offer a more realistic representation, by including other elements, especially parasitic resistors added as lumped elements connected both in series and/or in parallel to account for the possible presence of significant ohmic losses, as indicated in Figs. 1(b), (c) and (d). Similarly, and in order to be able to better account for the possible presence of more than one significant junction conduction mechanism, the equivalent circuit might also need to include more than one diode connected in parallel with the photo-current source, as presented in Fig. 1(e).

Relevant lumped parameters potentially introduced in these more complex equivalent circuit models, in addition to the value(s) of the series R_S and shunt R_P=1/G_P resistors, are the magnitudes I_{01} , I_{02},... of the reverse saturation current(s) and the corresponding value(s) of the junction ideality factor(s) n_1, n_2,... of the possible multiple diodes needed.

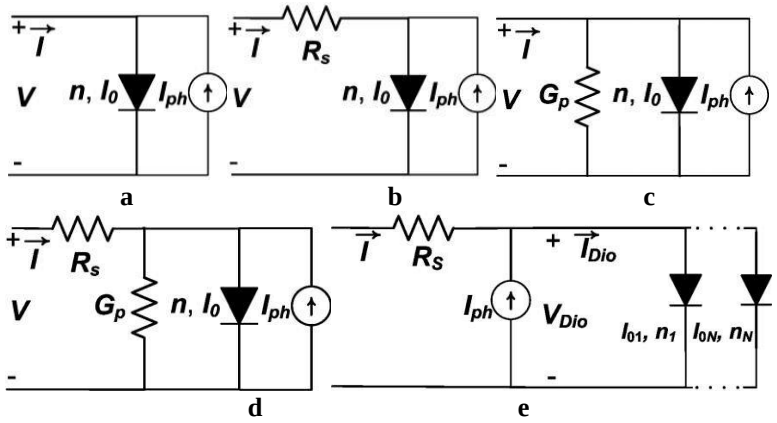

Fig. 1 Typical generic solar cell dc lumped-parameter equivalent circuit models showing the photo-generated current source with: (a) a single ideal diode in parallel; (b) plus a series resistance; (c) plus a parallel conductance; (d) plus both series resistance and parallel conductance; and (e) several ideal diodes plus a series resistance.

The parameters that may be used are supposed to bear direct associations to relevant fundamental microscopic physical features and phenomena actually present in the real solar cell to be modelled.

The various circuit elements added to the basic dc equivalent circuit model of Fig. 1(a) undoubtedly improve the model's descriptive fidelity. However, their presence, as shown in Figs. 1(b), (c), (d) and (e) also fundamentally complicates the mathematical handling of the resulting descriptive *I*-*V* equations. Because of them the basic equation ceases to be explicit to become an implicit transcendental equation. From the point of view of photovoltaic system simulation and solar cell model parameter extraction through curve fitting, being transcendental is an undesirable trait of the descriptive equations. Except in very few specific cases, they cannot be explicitly solved for the terminal current as a function of the terminal voltage, and vice versa, using only elementary functions.

2.2. Conventional models' mathematically descriptive equations and their solutions

Luckily, there is the Lambert*W* function, which we will refer to here as *W* for short. This function comes in very handy for explicitly solving equations which are made up of both linear and exponential terms, such as those equations that describe the circuits of Figs. 1(b), (c), and (d).

This special function *W*, whose utility was ignored to a large extent until not long ago, may be succinctly defined as the solution to the generic linear-exponential equation: $z = W(z)\, e^{W(z)}$, where z is any complex number [13, 14]. Around the turn of this century the use of *W* started to become an accepted and increasingly ubiquitous tool for solving various important problems of physics [15, 16]. The problems newly solved by using *W* prominently include important areas related to semiconductor physics, such as electronic devices and circuits, where linear-exponential type of equations abound since they play essential roles in describing the underlying phenomenology. Numerical calculation of *W* is relatively transparent nowadays, since various methods exist to quickly compute the principal $W_0(z)$ and other branches of *W*. Additionally, efficient algorithms are routinely implemented in most major mathematical software packages, physics and device modelling tools, and circuit simulation systems.

At the turn of the century two seminal works dealing with the use of *W* in the field of electronic circuit problems were published in the year 2000. One was an exact *W*-based analytical solution, proposed by Banwell and Jayakumar [17], of the terminal current *I* as an explicit function of the terminal voltage *V* for Shockley's modified equation [12]. It describes a circuit consisting of the series combination of a single diode and a lone resistor R_S (similar the circuit of Fig. 1(b) less the current source) which is expressed as:

$$I = I_0 \left[\exp\left(\frac{V - IR_S}{nv_{th}} \right) - 1 \right], \tag{1}$$

where I_0 is the reverse saturation current of the diode, $v_{th} = k_B T/q$ is the thermal voltage and n is the so-called diode ideality factor, which describes how much the diode's junction carrier transport mechanisms deviate from supposedly "ideal" behaviour (n=1). The exact *W*-based analytical solution of the terminal current as an explicit function of the terminal voltage presented by Banwell and Jayakumar is [17]:

$$I = \frac{nv_{th}}{R_S} W_0\left[\frac{I_0 R_S}{nv_{th}} \exp\left(\frac{V + I_0 R_S}{nv_{th}}\right)\right] - I_0 . \tag{2}$$

Because only a series-connected resistor was assumed to be involved in this problem, just the terminal current I needs be explicitly solved using W; whereas the terminal voltage V can be directly expressed as an explicit function of the terminal current using the natural logarithm elementary function:

$$V = nv_{th} \ln\left(\frac{I + I_0}{I_0}\right) + IR_S . \tag{3}$$

The other contemporaneous turn of the century seminal work about the use of W in the field of electronic circuit problems was published by Ortiz-Conde et al also in 2000 [18]. It was more comprehensive in the sense that it also contemplated the presence of significant shunt conductance $G_P=1/R_P$. This seminal work presented the derivation of the two exact W-based analytical solutions for both the terminal current and the terminal voltage as explicit functions of each other, of the transcendental equation corresponding to the circuit composed of a single diode and both series- and shunt-connected resistors, R_S and R_P, respectively (similar to the circuit of Fig. 1(d) less the current source). Shockley's modified terminal current equation in this case has an extra implicit term that accounts for the additional shunt conductance:

$$I = I_0\left[\exp\left(\frac{V - IR_S}{nv_{th}}\right) - 1\right] + \frac{V - IR_S}{R_P} . \tag{4}$$

The explicit W-based closed form analytic solutions for both I and V as explicit functions of each other, as presented by Ortiz-Conde et al [18] are, for the current:

$$I = \frac{V}{R_S} + \frac{nv_{th}}{R_S} W_0\left[\frac{I_0 R_S}{nv_{th}(R_S G_P + 1)} \exp\left(\frac{V + I_0 R_S}{nv_{th}(R_S G_P + 1)}\right)\right] - \frac{V + I_0 R_S}{R_S(R_S G_P + 1)} , \tag{5a}$$

or $$I = \frac{V}{R_S} - \frac{nv_{th}}{R_S} \ln\left\{\frac{nv_{th}(R_S G_P + 1)}{I_0 R_S} W_0\left[\frac{I_0 R_S}{nv_{th}(R_S G_P + 1)} \exp\left(\frac{V + I_0 R_S}{nv_{th}(R_S G_P + 1)}\right)\right]\right\}; \tag{5b}$$

and for the voltage:

$$V = IR_S + nv_{th} W_0\left[\frac{I_0}{nv_{th} G_P} \exp\left(\frac{I + I_0}{nv_{th} G_P}\right)\right] + \frac{I + I_0}{G_P} , \tag{6a}$$

or $$V = IR_S + nv_{th} \ln\left\{\frac{nv_{th} G_P}{I_0} W_0\left[\frac{I_0}{nv_{th} G_P} \exp\left(\frac{I + I_0}{nv_{th} G_P}\right)\right]\right\}. \tag{6b}$$

It might be noticed that eliminating the shunt conductance loss (letting $G_P=1/R_P \to 0$) does revert (5) back into (2), as it should, but does not allow to directly convert (6) into (3).

Four years after the publication of these two important seminal works about how to use *W* to derive exact explicit solutions for both *I* and *V* of a circuit consisting of a (dark) diode with series- and parallel resistors, Jain and Kapoor illuminated in 2004 the previously dark circuit model by adding in parallel with the diode a current source of a photo-generated intensity I_{ph} [19]. By so doing, the previously dark circuit became the illuminated solar cell equivalent circuit model shown in Fig. 1(d).

The new constant current concisely represents the photo-current I_{ph} generated by the transport and collection of separated charge carriers that are photo-generated within the cell's body by the absorption of sufficiently energetic incoming photons that penetrate through the diode's illuminated surface (now a photovoltaic diode). This photo-current must be inserted as an additional constant current term into the descriptive equation (4), so that now under illumination (4) becomes:

$$I = I_0\left[\exp\left(\frac{V - IR_S}{nv_{th}}\right) - 1\right] + \frac{V - IR_S}{R_P} - I_{ph}\,. \tag{7}$$

The addition of the constant to transcendental Eq. (4) does not alter the manner Eq. (7) is solved, which remains the same as it was for Eq. (4) [18].

The resulting exact *W*-based analytical solutions for both the terminal current and the terminal voltage, as explicit functions of each other, published in 2004 by Jain and Kapoor [19], are similar to Eqs. (5) and (6), except for the presence of the added I_{ph} term. For the current:

$$I = \frac{V}{R_S} + \frac{nv_{th}}{R_S} W_0\left[\frac{I_0 R_S}{nv_{th}(R_S G_P + 1)} \exp\left(\frac{V + (I_0 + I_{ph})R_S}{nv_{th}(R_S G_P + 1)}\right)\right] - \frac{V + (I_0 + I_{ph})R_S}{R_S(R_S G_P + 1)}\,, \tag{8a}$$

or

$$I = \frac{V}{R_S} - \frac{nv_{th}}{R_S} \ln\left\{\frac{nv_{th}(R_S G_P + 1)}{I_0 R_S} W_0\left[\frac{I_0 R_S}{nv_{th}(R_S G_P + 1)} \exp\left(\frac{V + (I_0 + I_{ph})R_S}{nv_{th}(R_S G_P + 1)}\right)\right]\right\}; \tag{8b}$$

and for the voltage,

$$V = IR_S - nv_{th} W_0\left[\frac{I_0}{nv_{th} G_P} \exp\left(\frac{I + I_0 + I_{ph}}{nv_{th} G_P}\right)\right] + \frac{I + I_0 + I_{ph}}{G_P}\,, \tag{9a}$$

or

$$V = IR_S + nv_{th} \ln\left\{\frac{nv_{th} G_P}{I_0} W_0\left[\frac{I_0}{nv_{th} G_P} \exp\left(\frac{I + I_0 + I_{ph}}{nv_{th} G_P}\right)\right]\right\}. \tag{9b}$$

Therefore, having inserted the additional photocurrent term I_{ph} into Eqs. (5) and (6), they have become the *W*-based solutions (8) and (9) which explicitly describe the electric behaviour of illuminated solar cells with significant series and shunt parasitic resistances.

It is interesting to check that turning the light off (by letting $I_{ph} \to 0$) reverts Eqs. (8) and (9), as they should, back into the original Eqs. (5) and (6), respectively. One year later, in 2005, Jain and Kapoor directly used these same *W* function-based solutions, corresponding to the conventional solar cell lumped-parameter equivalent circuit model of Fig. 1(d), to study organic solar cells [20].

In addition to a significant presence of both series and shunt parasitic resistances, sometimes it is evident in the measured *I-V* characteristics of the solar cell the presence of more than one significant conduction mechanism. In such cases multiple-diode equivalent circuit models are called for. They contain more than just one diode in parallel with the photocurrent source, as shown in Fig. 1(e). Consequently, the corresponding equations turn out to be of a multi-exponential nature and, thus, are in general more difficult, or even impossible, to solve exactly in an explicit form. Regardless of the difficulty, such type of multiple-diode equivalent circuits must be used whenever the presence of multiple junction conduction mechanisms must be adequately described because their relative significance so demands [21, 22].

For a complete review of the existing literature about generic solar cell dc lumped-parameter equivalent circuit models and their corresponding equations, solutions, and methods for numerically extracting their parameters, see Refs. [1, 23-26] and the references cited therein.

Although most solar cells can be adequately described by one of the just mentioned generic lumped-parameter equivalent circuit models, some researchers still prefer to use other models that are specifically intended for particular types of solar cells. For example, J. W. Jin, et al recently published a universal compact model for organic solar cells, which consists of individually describing three different regimes of operation and then combining their mathematical descriptions into a single equation [27]. Unfortunately, even that universal model for organic solar cells is not capable of describing the concave S-shaped behaviour occasionally exhibited by the illuminated *I-V* characteristics of organic solar cells.

In fact, none of the just described conventional dc lumped-parameter equivalent circuit models seem to be capable by itself of properly modelling the occurrence of the undesirable S-shaped behaviour observed in the illuminated *I-V* characteristics of several types of solar cells [28, 29]. Consequently, more suitable specialized circuit models need to be introduced to specifically represent the S-shaped kink. In the following sections we will analyse the issue of how to best describe, through other dc lumped-parameter equivalent circuit models, the harmful S-shaped deformation of the illuminated *I–V* characteristics, whose presence might seriously spoil the energy conversion performance of solar cells, especially but not exclusively those of organic solar cells [7].

3. THE S-SHAPE KINK

As already mentioned above, some promising important types of solar cells can, and do, under certain circumstances exhibit the undesirable S-shaped concave deformation of their illuminated *I-V* characteristics. The S-shape kink is most evident in the fourth quadrant, where it can seriously reduce the fill factor, and thus, impair the solar energy conversion efficiency of the device. Therefore when this is the case, corrective or palliative measures must be adopted to avoid or suppress the emergence of this detrimental kink.

Many researchers have proposed several explanations of the probable causes of this S-shaped concavity, but its origins are still not totally clear. Materials-related charge transport restrictions and charge accumulation-related interface phenomena, which alter the distribution of the solar cell's internal electric field are generally regarded to be mainly

responsible for the occurrence of the S-shaped kink [5, 7, 11, 30-33]. In organic solar cells, misaligned metal work functions and selective blocking contacts can produce injection barriers, and insulating interfacial layers between the metal and the active layers can produce extraction barriers, both of which might produce the fatidic S-shape [34].

Similar more or less pronounced S-shapes also can be observed in the measured characteristics of many types of experimental and developmental photovoltaic devices. For example, transient forward, or even reverse, $I-V$ sweeps of perovskite semiconductor-based solar cells, where both ion migration and mobile charge trapping seem to cause undesirable scan direction-dependent hysteresis in their illuminated *I-V* curves [4, 5]. The same kind of S-shaped kink also has been observed in a-Si/c-Si hetero-junction solar cells at certain temperature and illumination levels [2].

Other types of emerging more exotic photovoltaic devices display this type of detrimental behaviour. That is the case, for example, of the novel experimental ultra-thin photovoltaic cells made with Van der Waals force-bonded hetero-structures containing atomically thin layers of semiconducting transition metal dichalcogenides (such as MoS_2, WS_2 and WSe_2) [35]. Their illuminated *I-V* curves also exhibit detrimental S-shaped deformations that need to be suppressed for this attractive type of device to ever achieve usable energy conversion efficiency levels.

It is, therefore, essential to identify the possible origins of the S-shape kink if we pretend to avoid or diminish it. Thus, identifying and understanding the origin(s), as well as quantifying their influence on the S-shape kink's emergence, growth or suppression, becomes a crucial task for optimising the design of such solar cells. This goal may be conveniently achieved through the introduction of additional lumped elements into an existing conventional solar cell equivalent circuit model, to modify it so that it may electrically account for the full range of illuminated *I-V* characteristics, especially including the S-shaped kink behaviour.

This was kind of analysis followed by L. Zuo, et al, among others, for investigating the origin of the S-shaped kink in the *I-V* characteristics of organic solar cells [36], who use an equivalent circuit model approach [37] as a tool for analysis. The object of study then becomes the evolution of the solar cell's *I-V* characteristics experimentally measured under different operating conditions (illumination intensity, temperature, etc), or in response to adjustments in material composition, morphology, structural design and fabrication specifications, etc. The analysis of how the equivalent circuit's lumped-elements' parameter values (as extracted by fitting the model's equations to the measured data) change in response to modifications of the conditions, can be used as a powerful tool to scrutinise and understand the causes of the S-shape kink, and, thus, to learn how it may be best suppressed.

4. EQUIVALENT CIRCUIT MODELLING OF THE S-SHAPE KINK

Many solar cells unfortunately exhibit this undesirable S-shaped "kink" visibly in the fourth quadrant of their illuminated *I-V* characteristics. Since the kink cannot be described using only the conventional dc lumped-parameter equivalent circuit models shown in Fig. 1, and discussed in the preceding sections, ancillary circuits have been proposed for over a decade [28, 29]. The additional lumped elements must be incorporated together with a

conventional dc lumped-parameter equivalent circuit model to offer an overall description of the illuminated *I-V* characteristics.

4.1. Model by B. Mazhari (2006)

As early as 2006 Mazhari already understood the incapacity of stand-alone existing conventional dc lumped-parameter equivalent circuit models for properly describing the measured *I-V* characteristics of some illuminated organic solar cells [38]. He suggested that the commonly held hypothesis that the photo-current of organic solar cells remains essentially constant throughout the whole fourth quadrant ($0<V<V_{OC}$) of operation, might not be such an adequate assumption, at least for some photovoltaic devices including organic cells. As a matter of fact, it is not hard to envision how assuming a non-constant (within $0<V<V_{OC}$) and suitably S-shaped voltage-dependent photo-current added in parallel with the dark diode could indeed suffice to produce a correct concave S-shaped behaviour, as that observed in measured *I-V* characteristics [28, 29].

Based on that idea, Mazhari proceeded to attempt to improve a conventional dc lumped-parameter equivalent circuit model by transforming it in such a way that it would also be capable of describing the S-shaped kink observed in organic cells [38]. The basic schematic diagram of the lumped-parameter equivalent circuit model proposed by Mazhari is shown in Fig. 2, where I_R, I_E and I_D account for recombination, extraction and dark currents, respectively.

In that circuit, the non-constant photo-generated current is modelled by the parallel combination of a constant current source and the recombination diode. Applying Kirchhoff's current law at nodes A and B, the following Eqs. (10) and (11) are obtained:

$$I_E = I_{ph} - I_R \,, \tag{10}$$

and

$$I = I_D - I_E \,. \tag{11}$$

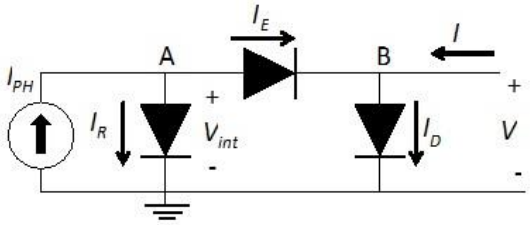

Fig. 2 DC lumped-parameter equivalent circuit model proposed by Mazhari [38] to describe the illuminated *I-V* characteristics of organic solar cells considering a non-constant photo-generated current.

Substituting Shockley's ideal current equation of every diode in Eqs. (10) and (11), and eliminating V_{int} yields the transcendental equation:

$$I_{ph} = I_{D0}e^{\alpha_D V} - I_{D0} - I + I_{R0}\left\{\left[I_{E0} + I_{D0}(e^{\alpha_D V} - 1) - I\right]\frac{e^{\alpha_E V}}{I_{E0}}\right\}^{\alpha_R/\alpha_E} , \tag{12}$$

where $\alpha_x^{-1} = n_x v_{th} = n_x k_B T/q$, and x means D, E, or R.

When the ratio α_R/α_E is a rational number, i.e. $\alpha_R/\alpha_E = a / b$, Eq. (12) becomes a polynomial equation that can be analytically solved for certain cases.

4.2. First model by F. Araujo de Castro et al (2010)

F. Araujo de Castro et al [10] proposed in 2010 to combine in series a conventional solar cell dc lumped parameter equivalent sub-circuit model with another sub-circuit that would specifically represent the S-shaped concave curve anomaly visible in the fourth quadrant of some illuminated *I-V* characteristics. Such series combination stems from the simple idea of describing the nonlinear (rectifying) contact behaviour observed in experimental diodes and photocells by means of an opposite-polarity series-connected lossy junction, frequently represented by a Shottky barrier with a shunt resistor. The diagram of the combined equivalent circuit model proposed by F. Araujo de Castro et al [10] is shown in Fig. 3.

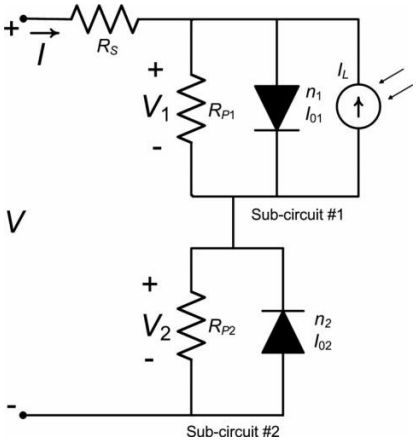

Fig. 3 Solar cell dc lumped-parameter equivalent circuit model proposed by Araujo de Castro et al [10] to describe the S-shaped kink. It includes a conventional single ideal diode with series and shunt resistances (sub-circuit #1) and series-connected sub-circuit #2 consisting of a single ideal diode and a parallel resistor to model the S-shaped kink

In addition to a conventional solar cell lumped-parameter equivalent circuit model (sub-circuit #1), comprised of a single diode with series (R_S) and shunt (R_{P1}) resistors, similar to that of Fig. 1(c), the modified equivalent circuit model includes an additional series-connected sub-circuit #2, that consists of a parallel combination of a second diode, with opposite polarity to that of the first diode, and a resistor R_{P2}, as shown in Fig. 3.

This additional sub-circuit#2 is the part of the total circuit whose function is to represent the experimentally observed detrimental S-shaped concave region of the illuminated *I-V* curve.

It could be easily demonstrated that, even using the *W* function, it is not possible to write, as would be desirable, an exact closed form mathematical expression of the terminal current as an explicit function of the terminal voltage of this series combination

of the two sub-circuits shown in Fig. 3. However, recalling the several generic solar cell dc lumped-parameter equivalent circuit models shown in Fig. 1, whose exact explicit solutions in terms of the *W* function we already know, it is easy to see that an exact solution must exist for the terminal voltage, *V*, as an explicit function of the terminal current *I* of this equivalent circuit model proposed by Araujo de Castro et al in 2010 [10].

The exact closed form analytical solution, which uses the *W* function, was first proposed by Romero et al [39]. As mentioned above, it is the solution for the equivalent circuit's terminal voltage *V* as a function of the terminal current *I*, and it is the only possible exact solution of this model. It consists of the sum of the voltage drop IR_S across the series resistor R_S and the voltages V_1 and V_2 across the terminals of each of the two sub-circuits, themselves expressed as exact explicit functions of the terminal current *I* using the *W* function:

$$V = IR_S + V_1 + V_2 , \tag{13}$$

where

$$V_1 = (I + I_{01} + I_{ph})R_{P1} - n_1 v_{th} W_0 \left\{ \frac{I_{01} R_{P1}}{n_1 v_{th}} \exp\left[\frac{R_{P1}}{n_1 v_{th}} (I + I_{01} + I_{ph}) \right] \right\}, \tag{14}$$

and

$$V_2 = (I - I_{02})R_{P2} - n_2 v_{th} W_0 \left\{ \frac{I_{02} R_{P2}}{n_2 v_{th}} \exp\left[\frac{R_{P2}}{n_2 v_{th}} (I - I_{02}) \right] \right\}. \tag{15}$$

The solution represented by the above system of three equations may be compacted for convenience into a single equation by adding (14) and (15) as in (13). Further simplification using the identity: $\ln(z)\text{-}W_0(z) = \ln[W_0(z)]$ that results from taking natural logarithms of the $W(z)$ definition [13], and after some term collection yields:

$$V = IR_S + v_{th} \ln\left\{ \frac{\left[\frac{n_1}{I_{01} R_{P1}} W_0 \left\{ \frac{I_{01} R_{P1}}{n_1 v_{th}} \exp\left[\frac{R_{P1}}{n_1 v_{th}} (I + I_{01} + I_{ph}) \right] \right\} \right]^{n_1}}{\left[\frac{n_2}{I_{02} R_{P2}} W_0 \left\{ \frac{I_{02} R_{P2}}{n_2 v_{th}} \exp\left[\frac{R_{P2}}{n_2 v_{th}} (I - I_{02}) \right] \right\} \right]^{n_2}} \right\}. \tag{16}$$

Roberts and Valluri have alerted about the possibility of arithmetic overflow when Eq. (13) with the ancillary Eqs. (14) and (15), or formula (7), are used for calculations [40]. Even quadruple floating point arithmetic can be insufficient to avoid overflow during calculations using certain parameter values. Hence, to avoid the risk of numerical overflow in the calculation they advise to rewrite the solution using the $g(x)$ function:

$$g(x) = \ln[W_0(e^x)] = x - W_0(e^x) . \tag{17}$$

Having at our disposal only the explicit solution for the voltage might constitute a small practical limitation of this model. However, it should not be really regarded as an important drawback, as alleged by Araujo de Castro et al [41], even when considering that most of the time solar cell characterisation is carried out by measuring the current while varying the voltage.

The exact explicit analytic solution for the voltage (16) for this lumped-parameter equivalent circuit model is still a very important contribution because, in addition to providing a one-equation formula for the *V-I* relation that eases its analytical manipulation, it also reduces the computation time needed for carrying out extensive simulations as compared to using raw implicit expressions.

Additionally, Eq. (16) substantially simplifies the burden of the numerical curve fitting needed for parameter extraction, even if an unusual numerical *V-I* curve-fitting "global lateral optimization" algorithm has to be utilized [21, 42].

This practical closed form explicit solution allowed Romero et al to easily run different simulations with various parameter values to investigate how the physical phenomena-related lumped-parameter components of sub-circuit #2 affect the S-shape and its evolution [39].

This dc lumped-parameter equivalent circuit model originally proposed by Araujo de Castro et al [10], and later explicitly solved by Romero et al [39], is able to adequately replicate up to V_{OC} ($I<0$; $0<V<V_{OC}$) the apparently anomalous concave behaviour that sometimes shows up in the fourth quadrant of illuminated *I-V* characteristics [43, 44]. K. Tada has recently proved this two diode model's validity for polymer cells under varying low level intensity illumination [45].

However, the same cannot be said of the shape of the illuminated *I-V* characteristic in the first quadrant above the open circuit voltage ($I>0$; $V>V_{OC}$), where the current yielded by this model is needlessly forced to level off, following a general trend imposed to a great extent by the *I-V* locus of R_{P2} (see dashed blue lines in Fig. 6). The reason is that in this model shown Fig. 3 the first quadrant is primarily dominated, for large forward voltages $>>V_{OC}$, by the linear parallel resistor R_{P2}, and thus, the *I–V* curve turns out to be quasi-linear. Instead, what seems to actually happen in real cells that exhibit these S-shape kinks, is that their *I-V* characteristic when measured under illumination in the first quadrant beyond the open circuit voltage ($I>0$; $V>V_{OC}$) at some point start to describe an upward turn and continue to grow in what appears to be an exponential-like fashion [7, 30, 31, 33].

This circuit has been successfully applied in different experiments that involve S-shaped removal with annealing [43] and UV soaking [46], and it has been validated with impedance measurements and ac modeling [47].

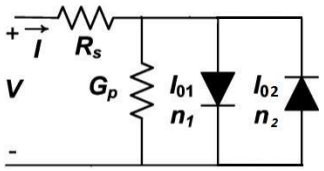

Fig. 4 DC lumped-parameter equivalent circuit model proposed by Gaur and Kumar [29] to describe the *I-V* characteristics of polymer solar cells under dark conditions. It looks almost like a conventional double diode with series and shunt resistances model, except that the diodes have opposite polarities.

4.3. Model by Gaur and Kumar (2013)

In 2013 Kumar and Gaur [28, 29] proposed an improved equivalent circuit model to represent the behaviour of polymer solar cells under different environmental conditions.

The proposed model does not result in a single compact formulation. The actual equivalent circuit turns out to be very complex and contains many circuit elements. The main reason for this is that the model itself separately treats the dark and illuminated characteristics, and even forward and the reverse characteristics are dealt with separately.

The proposed dark equivalent circuit is a parallel combination of a shunt resistor and two diodes connected with opposite polarity, all connected in series with a series resistor, as presented in Fig. 4. The dc equivalent circuit proposed to represent the *I–V* characteristics under illumination is based on the chief assumption that he photo-current is not constant but varies with applied voltage. It contains the dark circuit elements plus: a Zener diode, up to four more diodes, two photo-generated current sources, and additional unconventional resistors. It is shown in Fig. 1(b) of [28] and Fig. 7 of [29], but it is too complex to be of any practical use to reproduce here.

Although this model allowed Kumar and Gaur to understand the phenomenology of degraded P3HT: PCBM polymer solar cells, its complexity is such that it is not suggested as a practical compact equivalent circuit model to efficiently represent in general the S-shaped concave deformations that are observed under illumination in the *I-V* characteristics of some types of solar cells.

4.4. Model by F. J. García-Sánchez et al (2013)

To deal with the inability of the model by Araujo de Castro et al [10] shown in Fig. 3 to faithfully model real measured *I-V* data far beyond V_{OC}, a minor but crucial modification was introduced in 2013 by García-Sánchez et al [48]. The improvement affects the sub-circuit#2i part of the proposed equivalent circuit model diagram presented in Fig. 5.

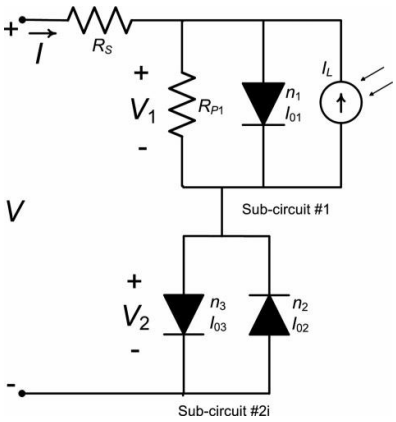

Fig. 5 The solar cell dc lumped-parameter equivalent circuit model proposed by García-Sánchez et al [48] to allow describing the S-shaped kink. It includes the same conventional single ideal diode with series and shunt resistances as before (sub-circuit #1), but the series-connected sub-circuit #2 has been modified to replace the previous resistor R_{P2} by a third diode connected with reversed polarity, the same as that of the diode of sub-circuit #1.

As in the model by Araujo de Castro et al [10], to reproduce the S-shaped concave region up to about the open circuit voltage ($I<0$; $0<V<V_{OC}$) the second sub-circuit of this model (sub-circuit#2i in Fig. 5) contains a second diode connected with reverse polarity relative to that of the first original diode in the conventional photovoltaic sub-circuit #1.

The difference here consists in that the resistor R_{P2}, which was connected in parallel with the second diode in sub-circuit #2 of Fig. 3, has been now removed and replaced by a third diode in sub-circuit#2i, connected in this case with the same forward polarity as that of the first original diode in the conventional photovoltaic sub-circuit #1. Thus, the second sub-circuit (sub-circuit #2i) has become an anti-parallel combination of diodes 2 and 3.

It is this third diode what allows the experimentally observed upturn of the illuminated *I–V* characteristics to show up in the first quadrant at voltage values beyond the open circuit voltage ($I>0$; $V>V_{OC}$). The substitution of the parallel resistor R_{P2}, by the third diode modifies the current through sub-circuit#2i, which now is:

$$I = -I_{02}\left[\exp\left(\frac{-V_2}{n_2 v_{th}}\right)-1\right]+I_{03}\left[\exp\left(\frac{V_2}{n_3 v_{th}}\right)-1\right]. \tag{18}$$

As before, we can write the solution for this equivalent circuit's terminal voltage V as a function of the terminal current I adding the voltage drop IR_S across the series resistor R_S and the voltages V_1 and V_2 across the terminals of each of its two sub-circuits, as in (13) which is repeated here:

$$V = IR_S + V_1 + V_2 . \tag{19}$$

However, now V_2 must be obtained by solving (18), and that solution is not explicit in general. It has close form *W*-based explicit solutions in some particular cases: that both ideality factors n_1 and n_2 are equal, or that one is twice as large as the other [48]. Otherwise, in general (18) would have to be solved numerically or approximately for the terminal voltage V_2. This is, of course, the price that must be paid for having a model with two diodes connected in parallel.

To illustrate the difference the addition of diode 3 makes regarding the description of the observed upturn of the illuminated *I–V* curve for $I>0$; $V> V_{OC}$, we present in Fig. 6 in in linear and semi-logarithmic scales the synthetic *I-V* characteristics of a hypothetical solar cell under illumination, as generated by numerical calculation using the two dc lumped-parameter equivalent circuit models (depicted in Figs. 3 and 5), with suitable parameter values indicated in the inset of Fig. 6 (b). Notice that in this particular example the two ideality factors n_1 and n_2 were chosen to have equal values, so that the solution for V_2 turns out to be explicit [48]. Therefore the terminal voltage V calculated from (19) is also an explicit function of the terminal current.

As can be seen in Fig. 6, the equivalent circuit models of Figs. 3 and 5 adequately describe, as expected, the S-shaped kink in the fourth quadrant of the illuminated *I–V* characteristics ($I<0$; $0<V<V_{OC}$). However, only the equivalent circuit model by García-Sánchez et al [48] (shown in Fig. 5), by virtue of the third diode in its sub-circuit#2i, is capable of appropriately describing an exponential-like upward bend in the first quadrant of the *I-V* characteristics beyond the open circuit voltage ($I>0$; $V>V_{OC}$).

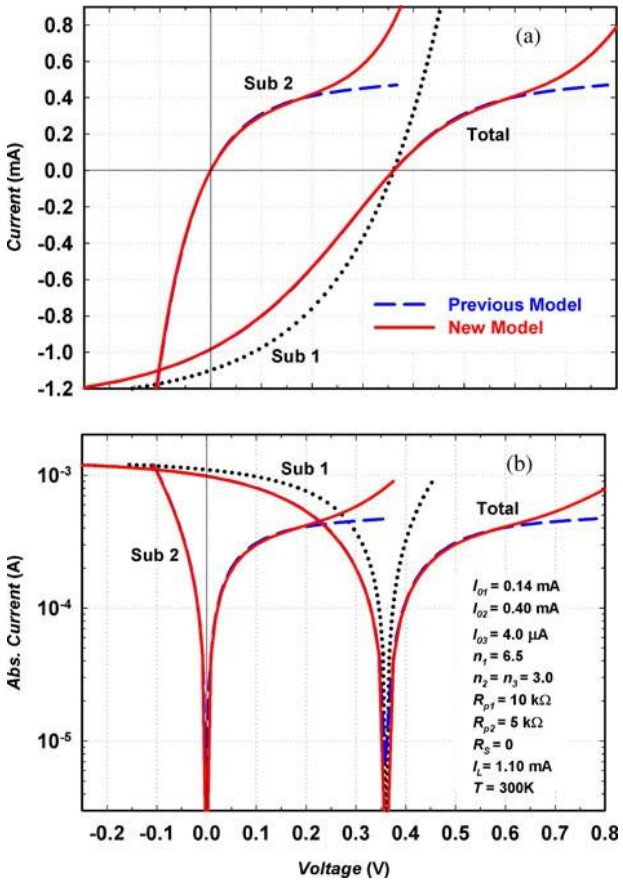

Fig. 6 Comparison of the S-shaped kinks in two synthetic illuminated *I-V* characteristics, presented in linear (a) and semi-logarithmic (b) scales, as generated by the dc lumped-parameter equivalent circuit models shown in Figs. 3 and 5, using the parameter values indicated within the lower pane (dotted black lines = sub-circuit #1, dashed blue lines = first model by Araujo de Castro et al [10], continuous red lines = model by García-Sánchez et al [48]).

The outstanding difference between both equivalent circuit models is easily visualised by comparing the dashed blue line and the continuous red line curves presented in Fig. 6, that correspond to *I-V* characteristics calculated with the model by Araujo de Castro et al [10] of Fig.3, and calculated with the model by García-Sánchez et al [48] of Fig.5, respectively.

As an example of a real exponential-like upward bend in the first quadrant of the *I-V* curve beyond the open circuit voltage ($I>0$; $V>V_{OC}$), data points corresponding to an experimental organic solar cell with S-shaped kink measured under arbitrary illumination and described in [48] are presented in Fig. 7.

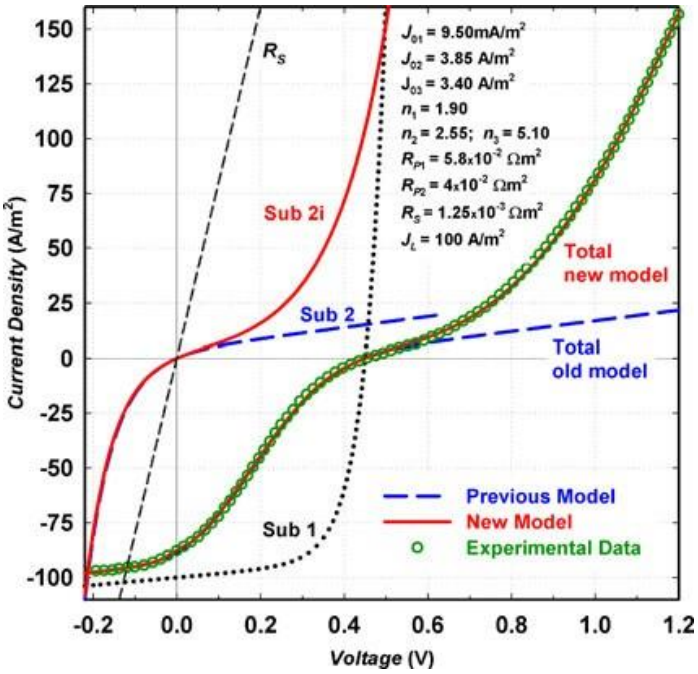

Fig. 7 Illuminated I-V characteristics of an experimental organic solar with S-shaped kink (dashed black straight line = Series Resistance *I-V* curve, dotted black line = sub-circuit #1 *I-V* curve, continuous dashed blue lines = sub-circuit #2 *I-V* curve and total model playback of previous model, red lines = sub-circuit #2i *I-V* curve and total model playback of newer model, green circles = measured *I-V* data).

Also shown in Fig. 7 is the playback calculated using the model by García-Sánchez et al [48] with the parameter values indicated in the figure which had been previously extracted by curve fitting of the model's equation to the originally measured data. Notice that in this case the relation $n_3=2n_2$ was imposed as a fitting condition, so that the solution for V_2 also turns out to be explicit [48], and the terminal voltage V calculated from (19) is also an explicit function of the terminal current.

Whenever the model's equations can be solved explicitly, we can avoid numerical iteration and thus ease the necessary curve fitting to experimental data when extracting the cell's model parameters. Such explicit equations are desirable also because they may be analytically operated on, which facilitates derivation of other analytic expressions, such as the temperature dependence of the open-circuit voltage.

For assessment purposes, Fig. 7 includes three separate *I-V* curves: two correspond to the conventional solar cell equivalent circuit model (sub-circuit #1), one is the R_S curve (black dash straight line), and the other (black dotted curve) corresponds to the parallel combination of the constant photo-current source, the first diode, and its companion shunt resistor R_{P1}. The third curve (continuous red line) corresponds to the S-shape-generating sub-circuit 2i, which is made up of the parallel combination of the second and third diodes with opposite polarities.

A quick look at the shapes of the curves in Fig. 7, in light of the terminal voltage equation (19) visually indicates how the S-shape kink is formed in the total model's *I-V* curve (shown in Fig. 7 on top of the green circles that represent the data points). In fact, the simple graphical addition of the three curves along the voltage axis, equivalent to adding the voltages across the three series-connected parts of the model (R_S, Sub-circuit 1 and sub-circuit 2i), confirms that the result is indeed a sort of double S shape, by virtue of the upward turn at its highest voltage end. Additionally, we may notice that the inflexion point of the shown total *I-V* curve is located at V_{OC}, as expected from the fact that the *I-V* characteristic of sub-circuit #2i, which is the anti-parallel combination of the two extra diodes, has its inflexion point at zero voltage.

It is worth mentioning at this point that the reason for proposing that a conventional solar cell equivalent circuit model be connected in series to an additional circuit with a configuration such as that of sub-circuit #2i, is not the result of an arbitrary attempt to try to empirically reproduce the observed upturn beyond V_{OC}. Rather, it is based on a certain understanding of how to best generalise the possible mechanisms that might be present in the different types of solar cells that exhibit this upturn beyond V_{OC}. Therefore, a configuration such as that of sub-circuit#2i is most probably justifiable as a reasonable circuital representation of specific underlying physical phenomena taking place near the interfaces of solar cells that display the S-shaped kink.

4.5. Model by L. Zuo et al (2014)

L. Zuo et al [36] proposed in 2014, an improved equivalent circuit model for Organic Solar Cells. They explain their proposal saying: "In view of the previous studies, an improved equivalent circuit is proposed to interpret the origin of S-shaped *I–V* curve and its effect on device performance." Their equivalent circuit model contains, as those proposed before, a sub-circuit with a rectifying junction connected in series with the conventional single-diode photovoltaic equivalent circuit, which is considered the essential reason for the S-shape curve. However, no mention is made in [36] of the previous models already proposed by Araujo de Castro [10] and García-Sánchez et al [48] in 2010 and 2013, respectively.

This sub-circuit is shown within the complete equivalent circuit model diagram presented in Fig. 8. Notice that there are two remarkable differences with respect to the original model by Araujo de Castro et al [10] (see Fig. 1(b) of [36]).The first and foremost is that the second diode in sub-circuit #2 is connected with the same forward polarity as the diode in the photovoltaic sub-circuit #1, whereas in the model proposed by Araujo de Castro et al [10] the second diode in sub-circuit #2 was connected with reverse polarity, opposite to that of the diode in the photovoltaic sub-circuit #1 (see Fig.3).

In this case the second diode is supposed to be a Schottky barrier junction introduced to represent the anode interface current caused by the rectifying properties induced by interfacial dipoles, unbalanced charge transport, etc. Nonetheless, it is noted that this model is not limited to the use of Schottky barriers, and thus any rectifying junction or non-Ohmic contact would do.

We must draw attention here to the fact that if an ideal diode with the same forward polarity as the photovoltaic diode were connected by itself (without R_{P2}) in series with sub-circuit #1 of Fig. 8, it would certainly modify the shape of the illuminated *I-V* curve

in the first quadrant, but at the same time it would suppress almost completely the current in the fourth quadrant. Therefore, if a significant (reverse) current is to flow through sub-circuit #2 under illumination, there must be substantial shunt current going around that second diode.

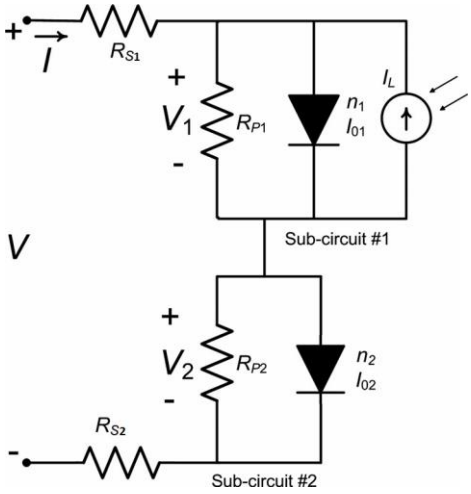

Fig. 8 Organic solar cell dc lumped-parameter equivalent circuit model proposed by Zuo et al [36] to describe the S-shaped kink. It includes the conventional single ideal diode with series and shunt resistances (sub-circuit #1), and series-connected sub-circuit #2 with a single Schottky diode and a parallel resistor, and additional series resistor.

That means that the value of the resistor R_{P2} that shunts the second forward diode in sub-circuit #2 (Fig. 8) must be small. We would like to mention in passing that a series combination of ideal diodes with equal polarity was used in the past to model amorphous silicon junctions [9].

The second difference introduced in this model is a minor one. It refers to the fact that now there is a second series resistor R_{S2}, in addition to R_{S1}, the already present series resistor of the model proposed by Araujo de Castro et al [10] (compare Figs.3 and 8). Although this second series resistor R_{S2} seems redundant, because from a circuits point of view it can be absorbed by R_{S1}, according to the explanation given in [36], this resistor "R_{s2} stands for the series resistance of each layer and interface resistance."

4.6. Second model by F. Araujo de Castro et al (2016)

Seeking further generalisation, Araujo de Castro et al published in 2016 [41] a modification of the previous model by García-Sánchez et al [48]. In fact, what they proposed is a generalised 3-diode model (shown in Fig. 9) aimed to, in these authors' own words, "gain insight into the modelling and parametrisation of organic solar cell current voltage curves" [41]. The modification introduced by Araujo de Castro et al consists of two specific changes that are made to the previous model.

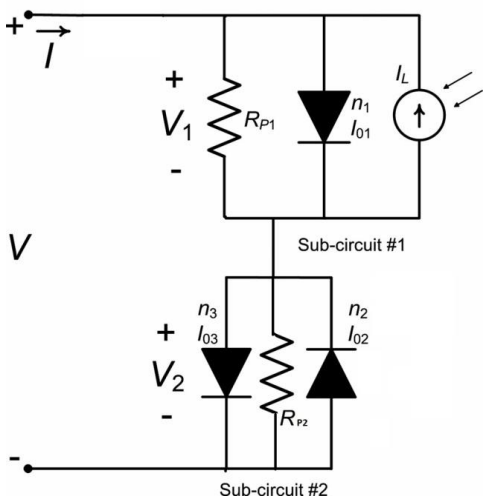

Fig. 9 Second solar cell dc lumped-parameter equivalent circuit model, proposed as an improvement by Araujo de Castro et al [41]. It is said to improve on the previous equivalent circuit model by García-Sánchez et al [48]. The previously present series resistor has been eliminated. The previously eliminated shunt resistor R_{P2} has been added again in parallel, but now with the two diodes in the series-connected sub-circuit #2

The first change made is the restoration of the shunt resistor R_{P2}, originally connected in parallel with the single diode of sub-circuit #2 in the first model by Araujo de Castro et al [10] shown in Fig. 3, which was later eliminated by García-Sánchez et al [48] to be replaced by a third forward polarity diode in anti-parallel connection with the second diode. That shunt resistor R_{P2} was restored Araujo de Castro et al [10], but it is now connected in parallel with the two diodes of sub-circuit 2i in the model by García-Sánchez et al [48] shown in Fig. 5. The second change made was to eliminate the series resistor R_S, which had been present in earlier equivalent circuit models.

The change in [41], that is, the restoration of the shunt resistor R_{P2}, seems to be a perfectly reasonable and necessary decision from a phenomenological point of view. The presence of that resistor R_{P2}, that was present in the first model by Araujo de Castro et al [10], and was then eliminated and replaced by a diode in the model by García-Sánchez et al [48], seems to be crucial for properly modelling bulk transport within the body of the solar cell.

From a graphical point of view, resistor R_{P2} controls the *I-V* curve's slope of sub-circuit #2i around the origin. At the same time, the presence within sub-circuit 2i of the third diode in anti-parallel connexion with diode 2 introduced by García-Sánchez et al [48] also seems to be necessary, in order to be able to produce the upward bend observed in the *I-V* curve beyond V_{OC}.

Therefore, the decision adopted in [41] of keeping both elements, the original shunt resistor R_{P2} and the third diode introduced in [Gar1348], seems to be the best way to address two physical phenomenon-related circuital issues that are not likely to be mutually

excluding, since one seem to come mainly from the bulk while the other probably of interfacial origin.

On the other hand, the second change made in [41] regarding the elimination of the series resistor R_S, which had been present in all earlier solar cell lumped-parameter equivalent circuit models, does not seem to be a convenient decision. In fact, from a methodological point of view, that series resistor R_S should not be even considered as part of the S-Shape-generating sub-circuit #2, but as part of the conventional solar cell circuit model. Therefore, there does not seem to be a good reason why R_S should be substantially altered when adding an S-Shape-generating sub-circuit to the total model.

To write the solution for this equivalent circuit's terminal voltage V as a function of the terminal current I only voltages V_1 and V_2 across the terminals of each of its two sub-circuits need be added, since R_S has been eliminated. Therefore, (19) becomes simply:

$$V = V_1 + V_2 \,. \tag{20}$$

However, now V_2 must be obtained by solving:

$$I = -I_{02}\left[\exp\left(\frac{-V_2}{n_2 v_{th}}\right)-1\right] + I_{03}\left[\exp\left(\frac{V_2}{n_3 v_{th}}\right)-1\right] + \frac{V_2}{R_{P2}} \,. \tag{21}$$

The solution of (21) is not explicit in general and would have to be solved numerically or approximately for the terminal voltage V_2.

4.7. Model by P. J. Roland et al (2016)

Regardless of the model development methodology used, the fact is that R_S represents an indispensable lumped element of any solar cell equivalent circuit model to be able to describe the presence of omnipresent parasitic resistance at the contacts and other collecting electrode resistance. Therefore, it is important keeping this series resistor R_S in place, in any solar cell dc lumped parameter equivalent circuit model.

The improved solar cell dc lumped-parameter equivalent circuit model, shown in Fig. 10 as suggested by P. J. Roland et al [50], is another step forward in the sequence of models previously proposed in [10, 41, 48]. The series resistor has been restored as an indispensable lumped element needed to describe the ubiquitous parasitic series resistances present in all solar cells.

As before, we would write the solution for this improved equivalent circuit's voltage V as a function of I by adding the voltage drop IR_S across the now restored series resistor R_S and the voltages V_1 and V_2 across the terminals of each of its two sub-circuits. That means using (15) instead of (16), and obtaining V_2 by solving (7) through numerical or approximate means. Sub-circuit #2 contains the parallel combination of shunt resistor R_{P2} and the anti-parallel pair of diodes 2 and 3.

P. J. Roland et al [50] used SPICE simulations of this equivalent circuit model to reproduce *I-V* plots with S-shaped deformation for studying the influence of changing the values of the circuit element's parameters on the shape of the resulting *I-V* curve.

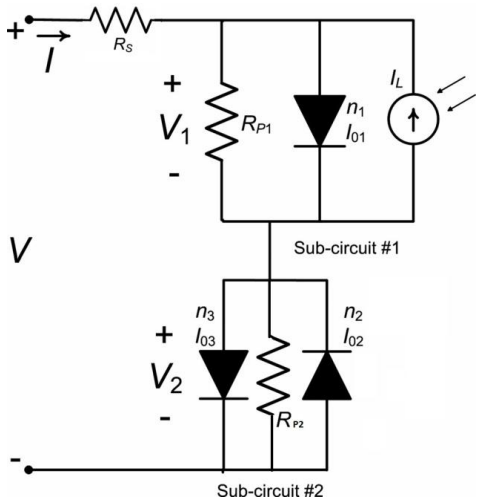

Fig. 10 An improved solar cell dc lumped-parameter equivalent circuit model, proposed by P. J. Roland et al [50] as a further improvement to the models proposed by Araujo de Castro et al [41] and by García-Sánchez et al [48]. The series resistor has been restored as a necessary element to describe the parasitic series resistance.

A comparison between experimentally measured data of CdS/CdTe/FeS_2 NC/Au photovoltaic devices at 200K, which exhibit S-shape kinks in the measured *I-V* characteristics and their corresponding simulated S-shaped curve was also carried out, trying to correlate the model's parameters with the physical features that determine current flow through the device.

5. CONCLUSION

We have presented a brief chronological review and appraisal of dc lumped-parameter equivalent circuits that have been proposed to date for modelling the effect of the S-shaped "kink" which shows up in the fourth quadrant, and eventually in the first, of the *I-V* characteristics measured under illumination of certain types of organic solar cells, as well as of some other types of photovoltaic devices. In doing so, we have analysed the defining mathematical equations of the available equivalent circuits, and we have provided and discussed their possible solutions. Critical analysis have been included and some recommendations were offered when relevant. We hope that the unifying approach and generic nature of this succinct review can provide extra insight and be of practical help to photovoltaic engineers and solar cell scientists that must deal with the important issue of the S-shape *I-V* curve deformation and its modelling through lumped-parameter equivalent circuits.

Acknowledgement: *Parts of his work were financially sponsored by the Madrid Autonomous Community and URJC, under projects Nos. S2009/ESP-1781 and URJC-CM-2010-CET-5173, respectively. Partial financial assistance was also received through an institutional grant from USB's Decanato de Investigación y Desarrollo.*

REFERENCES

[1] A. Ortiz-Conde, F. J. García-Sánchez, J. Muci, A. Sucre-González, "A review of diode and solar cell equivalent circuit model lumped parameter extraction," *Facta Universitatis, Series: Electronics and Energetic*s, vol. 27, no 1, pp. 57-102, March 2014.

[2] R. V. K. Chavali, J. V. Li, C. Battaglia, S. De Wolf, J. L. Gray, M. A. Alam, "A Generalized Theory Explains the Anomalous Suns–Voc Response of Si Heterojunction Solar Cells," IEEE Journal of Photovoltaics, vol. 7, no. 1, pp. 169 - 176, Jan. 2017.

[3] P. G. Kale, C. S. Solanki, "Silicon quantum dot solar cell using top-down approach." *International Nano Letters*, vol. 5, no. 2, pp. 61-65, Jun 2015.

[4] S. van Reenen, M. Kemerink, H. J. Snaith, "Modeling Anomalous Hysteresis in Perovskite Solar Cells," *J. of Phys. Chem. Letters*, vol. 6, pp. 3808−3814, 2015.

[5] F. Xu, J. Zhu, R. Cao, S. Ge, W. Wang, H. Xu, R. Xu, Y. Wu, M. Gao, Z. Ma, F. Hong, Z. Jiang, "Elucidating the evolution of the current-voltage characteristics of planar organometal halide perovskite solar cells to an S-shape at low temperature," *Solar Energy Materials & Solar Cells*, vol. 157, pp. 981–988, December 2016.

[6] J. Liu, G. Wang, K. Luo, X. He, Q. Ye, C. Liao, J. Mei. "Understanding the role of electron transport layer in highly efficient planar perovskite solar cells." *ChemPhysChem*. In Press, Jan 2017.

[7] A. Wagenpfahl, D. Rauh, M. Binder, C. Deibel, V. Dyakonov, "S-shaped current-voltage characteristics of organic solar devices," *Physical Review B*, vol. 82, no. 115306, September 2010.

[8] A. Opitz, R. Banerjee, S. Grob, M. Gruber, A. Hinderhofer, U. Hörmann, J. Kraus, T. Linderl, C. Lorch, A. Steindamm, A. K Topczak, "Charge Separation at Nanostructured Molecular Donor–Acceptor Interfaces," Chapter of *Elementary Processes in Organic Photovoltaics* , volume 272 of the series Advances in Polymer Science, pp. 77-108. Springer International Pub., 2017.

[9] V. H. Tran, R. B. Ambade, S. B. Ambade, S. H. Lee, I. H. Lee. "Low-Temperature Solution-Processed SnO_2 Nanoparticles as Cathode Buffer Layer for Inverted Organic Solar Cells." *ACS Applied Materials & Interfaces*, Accepted paper in press, Jan 2017.

[10] F. Araujo de Castro, J. Heier, F. Nüesch, R. Hany, "Origin of the Kink in Current-Density Versus Voltage Curves and Efficiency Enhancement of Polymer-C_{60} Heterojunction Solar Cells," *IEEE Journal of Selected Topics in Quantum Electronics*, vol. 16, no. 6, pp. 1690 – 1699, Nov/Dec 2010.

[11] B. Qi, J. Wang, "Fill factor in organic solar cells," *Phys.Chem. Chem. Phys.*, vol.15, pp. 8972-8982, 2013.

[12] W. Shockley, The theory of p-n junctions in semiconductors and p-n junction transistors, *Bell System Technical Journal*, vol. 28, no. 3, pp. 435−489, July 1949.

[13] R. M. Corless, G. H. Gonnet , D.E.G. Hare, D. J. Jeffrey, D. E. Knuth, "On the lambert w function." *Adv. Comput. Math*., vol. 5, no. 1, pp. 329–359, 1996.

[14] Lambert W-Function (4.13), NIST Digital Library of Mathematical Functions. http://dlmf.nist.gov/4.13

[15] S. R. Valluri, R. M. Corless and D. J. Jeffrey. "Some Applications of the Lambert W Function to Physics," *Canadian J. of Physics*, vol. 78, no. 9, pp. 823-831, 2000.

[16] D. Veberič, "Lambert W function for applications in physics," *Computer Physics Communications*, vol. 183, pp. 2622–2628, 2012.

[17] T. Banwell, A. Jayakumar, "Exact analytical solution for current flow through diode with series resistance." *Electronics Letters*, vol. 36, no. 4, pp. 291–292, 17 Feb. 2000.

[18] A. Ortiz-Conde, F. J. García-Sánchez, J. Muci, "Exact analytical solutions of the forward non-ideal diode equation with series and shunt parasitic resistances," *Solid-State Electronics*, vol. 44, no. 10, pp. 1861–1864, October 2000.

[19] A. Jain, A. Kapoor, "Exact analytical solutions of the parameters of real solar cells using Lambert W-function," *Solar Energy Materials & Solar Cells*, vol. 81, no. 2, pp. 269-277, February 2004.

[20] A. Jain, A. Kapoor, "A new approach to study organic solar cell using Lambert W-function," *Solar Energy Materials & Solar Cells*, vol. 86, pp. 197–205, 2005.

[21] D. C. Lugo-Muñoz, M. De Souza, M. A. Pavanello, D. Flandre, J. Muci, A. Ortiz-Conde, F. J. García-Sánchez, "Parameter Extraction in Quadratic Exponential Junction Model with Series Resistance using Global Lateral Fitting," *ECS Transactions*, vol. 31, no. 1, pp. 369-376, 2010.

[22] A. Ortiz-Conde, D. Lugo-Muñoz and F. J. García Sánchez, "An explicit multi-exponential model as an alternative to traditional solar cell models with series and shunt resistances," *IEEE Journal of Photovoltaics*, vol. 2, no. 3, pp. 261-268, July 2012.

[23] T. Ma, H. Yang, L. Lu, "Solar photovoltaic system modeling and performance prediction," *Renewable and Sustainable Energy Reviews*, vol. 36, pp. 304-315, 2014.
[24] V. J. Chin, Z. Salam, K. Ishaque, "Cell modelling and model parameters estimation techniques for photovoltaic simulator application: A review," *Applied Energy*, 154, pp. 500–519, 2015.
[25] A. M. Humada, M. Hojabri, S. Mekhilef, H. M. Hamada, "Solar cell parameters extraction based on single and double-diode models: A review," *Renewable and Sustainable Energy Reviews*, vol. 56, pp. 494–509, 2016.
[26] A. R. Jordehi, Parameter estimation of solar photovoltaic (PV) cells: A review," *Renewable and Sustainable Energy Reviews*, vol. 61, pp. 354–371, 2016.
[27] J. W. Jin, S. Jung, Y. Bonnassieux, G. Horowitz, A. Stamateri, C. Kapnopoulos, A. Laskarakis, S. Logothetidis, "Universal Compact Model for Organic Solar Cell," *IEEE Transactions on Electron Devices*, vol. 63, no. 10, pp. 4053-4059, October 2016.
[28] P. Kumar, A. Gaur, "Model for the J-V characteristics of degraded polymer solar cells," *Journal of Applied Physics*, vol. 113, no. 094505, 2013.
[29] A. Gaur, P. Kumar, "An improved circuit model for polymer solar cells," *Prog. Photovolt: Res. Appl.*, 2013.
[30] A. Kumar, S. Sista, Y. Yang, "Dipole induced anomalous S-shape I-V curves in polymer solar cells," *Journal of Applied Physics*, vol. 105, no. 094512, 2009.
[31] J. Wagner, M. Gruber, A. Wilke, Y. Tanaka, K. Topczak, et al, "Identification of different origins for s-shaped current voltage characteristics in planar heterojunction organic solar cells," *Journal of Applied Physics*, vol. 111, no. 054509, March 2012.
[32] R. Saive, C. Mueller, J. Schinke, R. Lovrincic, W. Kowalsky, "Understanding S-shaped current-voltage characteristics of organic solar cells: Direct measurement of potential distributions by scanning Kelvin probe," *Applied Physics Letters*, vol. 103, no. 243303, 2013.
[33] O. J. Sandberg, M. Nyman, R. Österback, "Effect of Contacts in Organic Bulk Heterojunction Solar Cells," *Phys. Rev. Applied*, vol. 1, 024003, 27 March 2014.
[34] W. Tress, O. Inganäs, "Simple experimental test to distinguish extraction and injection barriers at the electrodes of (organic) solar cells with S-shaped current–voltage characteristics," *Solar Energy Materials & Solar Cells*, vol. 117, pp. 599–603, 2013.
[35] M. M. Furchi, A. A. Zechmeister, F. Hoeller, S. Wachter, A. Pospischil, T. Mueller, "Photovoltaics in Van der Waals Heterostructures," *IEEE Journal of Selected Topics in Quantum Electronics*, vol. 23, no. 1, pp. 4100111, Jan/Feb 2017.
[36] L. Zuo, J. Yao, H. Li, H. Chen, "Assessing the origin of the S-shaped *I–V* curve in organic solar cells: An improved equivalent circuit model," *Solar Energy Materials & Solar Cells*, vol. 122, pp. 88–93, 2014.
[37] A. Cheknane, H. S. Hilal, F. Djeffal, B. Benyoucef, J.-P. Charles, "An equivalent circuit approach to organic solar cell modeling," *Microelectronics Journal*, vol. 39, pp. 1173–1180, 2008.
[38] B. Mazhari, "An improved solar cell circuit model for organic solar cells," *Solar Energy Materials & Solar Cells*, vol. 90, no. 7, pp. 1021-1033, May 2006.
[39] B. Romero, G. del Pozo, B. Arredondo, "Exact analytical solution of a two diode circuit model for organic solar cells showing S-shape using Lambert W-functions," *Solar Energy*, vol. 86, pp. 3026–3029, 2012.
[40] K, Roberts, S. R. Valluri. "On Calculating the Current-Voltage Characteristic of Multi-Diode Models for Organic Solar Cells." *arXiv preprint arXiv:1601.02679* , 2015.
[41] F. A. De Castro, A. Laudani, F. Riganti Fulginei, A. Salvini, "An in-depth analysis of the modelling of organic solar cells using multiple-diode circuits," *Solar Energy*, vol. 135, pp. 590–597, 2016.
[42] A. Ortiz-Conde, Y. Ma, J. Thomson, E. Santos, J. J. Liou, F. J. García-Sánchez, M. Lei, J. Finol, P. Layman, "Direct extraction of semiconductor diode parameters using lateral optimization method," *Solid-State Electronics*, vol. 43, no. 4, pp. 845–848, 1999.
[43] G. del Pozo, B. Romero, B. Arredondo, "Evolution with annealing of solar cell parameters modeling the S-shape of the current–voltage characteristic," *Solar Energy Materials & Solar Cells*, vol. 104, pp. 81–86, 2012.
[44] G. Del Pozo, B. Romero, B. Arredondo, "Extraction of circuital parameters of organic solar cells using the exact solution based on Lambert W-function," *Proceedings of the Int. Society for Optical Engineering (SPIE)*, Brussels, Belgium, vol. 8435, *Organic Photonics V*, 84351Z, June 2012.
[45] K. Tada, "Validation of opposed two-diode equivalent-circuit model for S shaped characteristic in polymer photocell by low-light characterization," *Organic Electronics*, vol. 40, pp. 8-12, 2017.
[46] B. Romero, G. Del Pozo, E. Destouesse, S. Chambon, B. Arredondo, "Circuital modelling of S-shape removal in the current–voltage characteristic of TiO_x inverted organic solar cells through white-light soaking," *Organic Electronics*, vol. 15, pp. 3546–3551, 2014.

[47] B. Romero, G. del Pozo, B. Arredondo, J. P. Reinhardt, M. Sessler, and U. Würfel, "Circuital Model Validation for S-Shaped Organic Solar Cells by Means of Impedance Spectroscopy," *IEEE Journal of Photovoltaics*, vol. 5, no. 1, pp. 234-237, January 2015.

[48] F. J. García-Sánchez, D. Lugo-Muñoz, J. Muci, A. Ortiz-Conde, "Lumped Parameter Modeling of Organic Solar Cells' S-Shaped *I-V* Characteristics," *IEEE Journal of Photovoltaics*, vol. 3, no. 1, pp. 330-335, January 2013.

[49] Ortiz-Conde, A., Estrada, M., Cerdeira, A., García Sánchez, F.J., De Mercato, G. , "Modeling real junctions by a series combination of two ideal diodes with parallel resistance and its parameter extraction," *Solid-State Electronics*, vol. 45, no. 2, pp. 223-228, 2001.

[50] P. J. Roland, K. P. Bhandari, R. J. Ellingson, "Electronic Circuit Model for Evaluating S-Kink Distorted Current-Voltage Curves," *Proc. IEEE 43rd Photovoltaic Specialists Conf. (PVSC),* 2016.